International Conference on Space Optics—ICSO 2022

Dubrovnik, Croatia

3–7 October 2022

Edited by Kyriaki Minoglou, Nikos Karafolas, and Bruno Cugny,

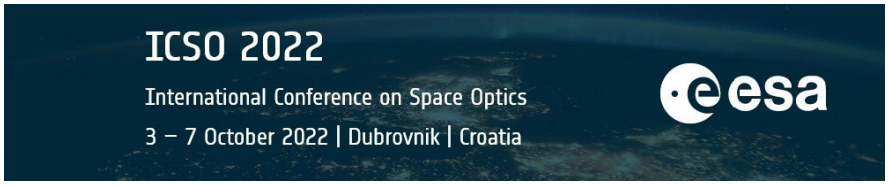

Development of a straylight diagnostics tool for the MOTA OGSE

International Conference on Space Optics — ICSO 2022, edited by Kyriaki Minoglou, Nikos Karafolas, Bruno Cugny, Proc. of SPIE Vol. 12777, 127775R · © 2023 ESA and CNES · 0277-786X · doi: 10.1117/12.2691038

Development of a straylight diagnostics tool for the MOTA OGSE

Mathieu Guilhem*[a] (Sophia Engineering), Laurie Capobianco-Peigné[a] (Sophia Engineering), Charlène Mercier[b] (Thales Alenia Space), Xavier Joffrin[b] (Thales Alenia Space).
[a]Sophia Engineering, 5 rue Soutrane, 06560 Sophia Antipolis, France;
[b]Thales Alenia Space, 5 allée des Gabians, 06150 Cannes, France.

ABSTRACT

Earth Observation instruments under ESA responsibility usually have very tight requirements concerning straylight performance. To quantify the straylight level of the instruments some dedicated Optical Ground Support Equipment (OGSE) are developed [1]. Particularly in the case of the MTG-FCI, the straylight is characterized using the MOTA (Multi Optical Test Assembly) OGSE [2] operated by Thales Alenia Space in Cannes, France. The acceptable FCI straylight level is very stringent thus it is important to ensure the level of straylight of such OGSE stays below a certain level. This paper presents a simple setup, inspired by the "external occultation coronagraph" architecture, capable of directly measuring the OGSE straylight level in typical NUST (Non-Uniform Scene Test) configuration.

Keywords: Straylight, diagnostics, MTG, FCI, OGSE

1. INTRODUCTION

One of the many characteristics that define the performances of a spaceborne imager is its straylight behavior. Straylight performance requirements can take various forms, but one commonly used metric is the luminance measured by the instrument in the dark section of a half-bright / half-dark scene. This test is usually referred to as a "Non-Uniform Scene Test" (NUST). In the presence of straylight, the dark half of the image will be polluted by light from the bright fields. In most of the case, the NUST scene is projected from a collimator-type OGSE with a suitable object at its focal plane.

This collimator OGSE has its own straylight performances, which raises an obvious issue: the straylight level seen on the focal plane of the instrument will be a combination of straylight generated inside the instrument and straylight generated inside the OGSE. The usual solution is to require that the OGSE straylight level is low or negligible compared to the instrument requirement. As instruments performance requirements increase, the corresponding constraints on the OGSE increase.

The next step of this problem is: how do we check that the OGSE straylight level is compliant? Testing would require a measurement device with a straylight level negligible compared to the OGSE specification; this instrument would need to be validated, and so on. The commonly used method to get out of this spiraling cycle is to verify the OGSE straylight compliance through indirect means: analysis coupled with optics roughness and contamination requirements.

The goal of the work presented here is to directly assess the straylight of an OGSE in a manner that guaranties a negligible contribution of the measurement device. The test case for the method is the MOTA OGSE, used by Thales Alenia Space France in Cannes to test various performances of the Flexible Combined Imager (FCI) instrument onboard Meteosat Third Generation (MTG) [2], [3].

One requirement on the FCI instrument [4],[5],[6],[7] is to have a straylight level inferior to 0.5% beyond 2.8mrad from black/white transition and inferior to 1% between 1.4mrad and 2.8mrad from this transition. In consequence, MOTA OGSE straylight requirement is to be inferior to 0.08% @1mrad from the transition.

The design of MOTA is optimized to minimize this straylight. No transmissive optics are used. The number of optical elements is limited. Roughness and contamination of mirrors are specified and controlled. MOTA is now manufactured.

*mathieu.guilhem@sophiaengineering.com

2. PRINCIPLE

Instrument straylight is typically assessed using high-contrast scenes composed of sharp transitions between a bright portion and a dark portion. In the "NUST" scene, half of the instrument's FOV is illuminated with radiance Lmax and the other half is illuminated with radiance Lmin. Lmin is usually theoretically zero, i.e. one half of the FOV is "dark". This scene is illustrated on Figure 2-1.

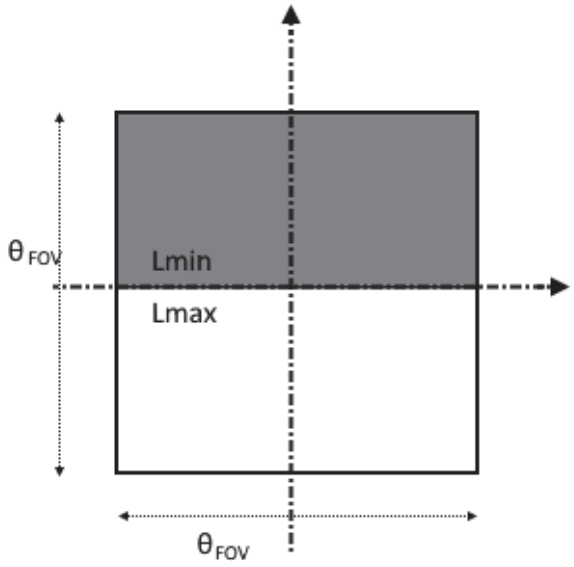

Figure 2-1 – Non uniform scene test (NUST)

Scatter and diffraction in the OGSE will induce pollution between the two areas which results in Lmin being unknown. In the instrument under test, the same phenomena will induce additional pollution, so that the radiance seen by the instrument in the "dark" area is different from Lmin.

We designed our measurement setup, the Straylight Bench (SLB), using inspiration from the field of coronagraphy where scenes are by nature of very high contrast. The well-known "Lyot coronagraph" architecture has stringent roughness and contamination constraints on the front optic, so we turned to an alternate design known as "external occultation". This design was first introduced by Evans (1948) but is commonly known as the "Newkirk coronagraph" after Gordon Newkirk who perfected the design in 1966. The Newkirk design was subsequently used in most spaceborne coronagraphs. An overview of the history of these instruments is presented in [8].

In the Newkirk design the bright light from the sun is blocked by the combination of a disk and a circular diaphragm placed in front of the imaging system. The imaging system itself includes the classical Lyot architecture. In this design most of the light from the sun is blocked before it can reach any optical element, thus relaxing the roughness and cleanliness requirements.

In designing the SLB we kept the idea of external occultation of the bright source but discarded the Lyot stop. This simplification is allowed by the fact that the bright-to-dark ratio, and thus the magnitude of the diffraction effects, is less severe in our case. A post-processing "software Lyot stop" method was designed to mitigate the diffraction contributors. The geometry of the occultation system was modified to be compatible with our scene, the NUST transition.

The principle is illustrated on Figure 2-2 for a single field point on each side of the transition, and Figure 2-3 for an extended NUST scene.

The principle is most clearly understood by looking at Figure 2-2 (left): light coming from any source point in the upper part of the scene is totally intercepted before it can enter the imager on the right. The absorption is due to the combination of the two occulters: on the figure it is seen that the first occulter absorbs only a portion of the green rays; the second

occulter absorbs the remaining portion. In contrast, light coming from the lower part of the scene, here in blue, is only partially absorbed by the two occulters. Note that in the lower part of the scene, due to the geometry of the system the partial absorption decreases as the source point gets further away from the optical axis.

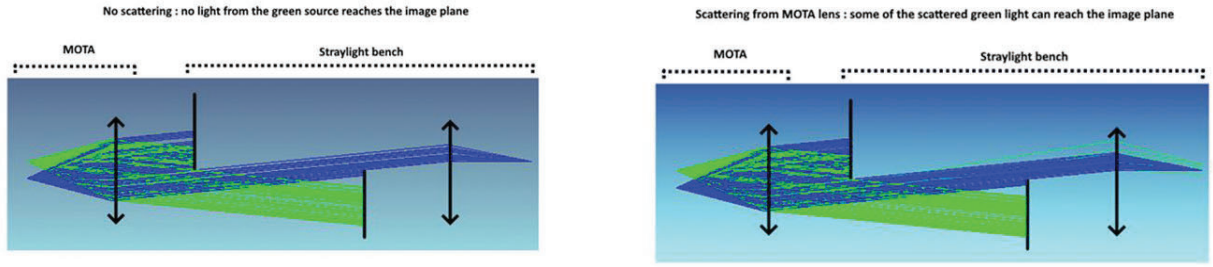

Figure 2-2 – SLB principle of operation. Left: no scattering in the OGSE. Right: scattering in the OGSE.

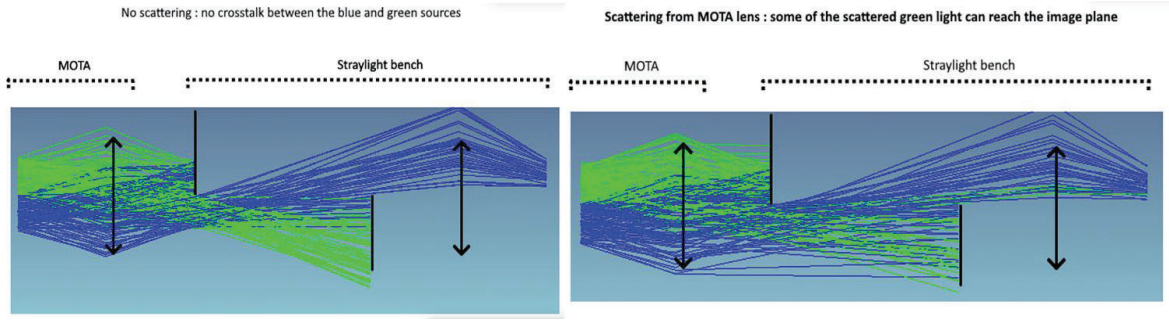

Figure 2-3 – SLB with an extended source. Left: no scattering in the OGSE. Right: scattering in the OGSE.

The green rays come from the bright (Lmax) half of the scene and the blue ones come from the dark (Lmin) half. In the ideal case (left column) the combination of the two occulters intercepts any high-radiance (green) rays. Only green rays scattered inside the OGSE (right column) can reach the SLB detector.

Since only OGSE straylight reaches the SLB's imager system, the sources of straylight internal to the bench's imager are negligible. Notably, the performances are largely insensitive to the particulate contamination of the SLB.

Additionally, behind the occulted area (bottom half of the SLB detector on the figures) the signal received by the detector can only originate from inside the SLB: the system has a built-in self-check.

3. USE CASE: MOTA

3.1. The MOTA OGSE

MOTA (Multi Optical Test Assembly), as seen in Figure 3-1, is one of the FCI (MTG) OGSE. MOTA is used for geometrical and straylight characterization in VNIR and IR as well as radiometric calibration in VNIR of the FCI. It produces objects at infinite via a High-Resolution Collimator and optical sources in VNIR (integrating sphere) and IR (Black Body). To produce the image of an object, the MOTA is composed of a pattern plate (Figure 3-2) containing several patterns: small square, small hole, large square, slits, grids. In this study, the large hole (LH in figure 3-2) has been used to align the setup and to perform the black and white transition.

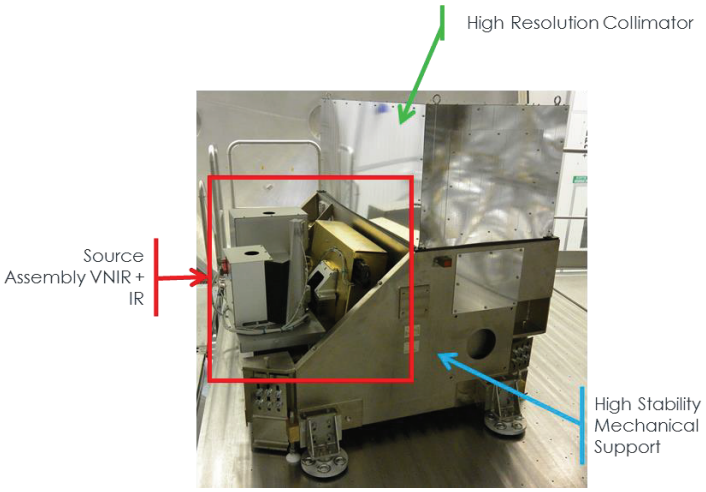

Figure 3-1 Instrument use case MOTA

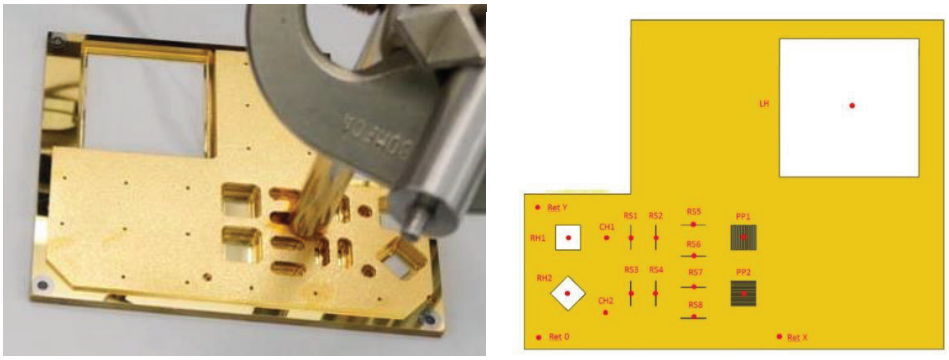

Figure 3-2 Pattern plate of MOTA

The main specification of MOTA is to provide image of objects on a field of view of +/-4.5mrad. The straylight requirement that has been defined for MOTA is quite stringent (<0.08% at 1mrad from the black/white transition). It has been defined at the beginning of the project and is much lower than the FCI straylight requirement.

3.2. SLB design

The SLB principle was adapted to the specific pupil size and field-of-view of MOTA. Since one of the goals of the project was to demonstrate a low-cost straylight measurement setup, usage of COTS was prioritized. As a result, the following choices were made:

- The imager is composed of a commercial telescope and a commercial Pelletier-cooled camera.
- The occulters are custom-made due to their unique geometry.
- All other mechanical parts (mechanical structure, component mounts, etc.) are COTS as much as possible.

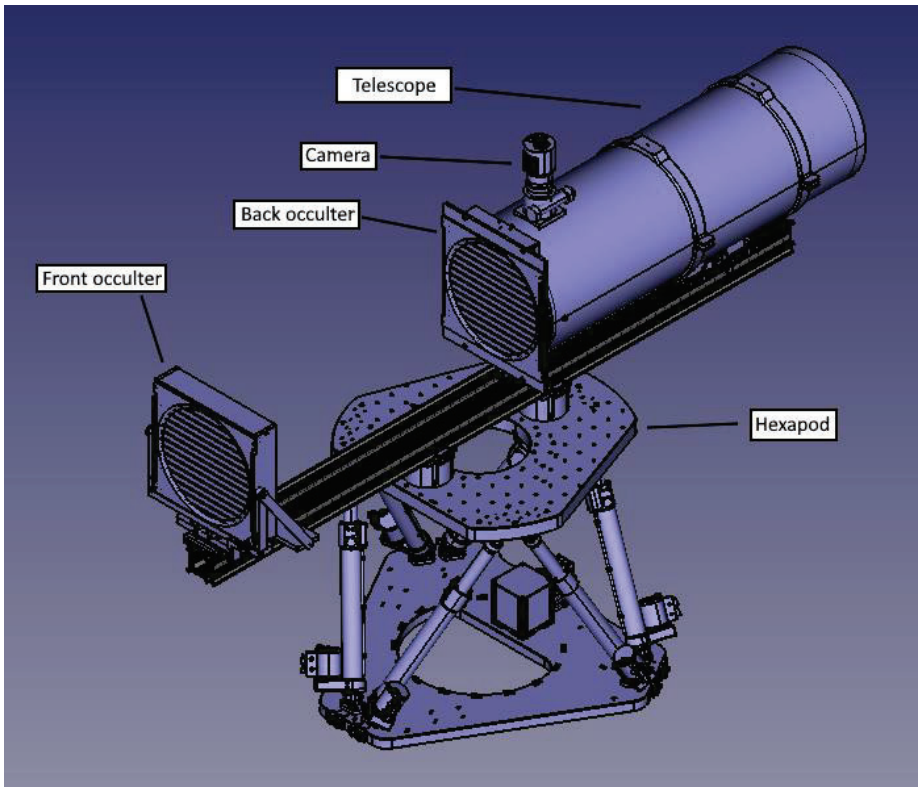

Figure 3-3 – Straylight bench design overview.

The setup (Figure 3-3) is 2.2m long (including 1m between the two occulters) by 1.5m high (including the hexapod) and weights 70kg (excluding the hexapod). The system's size was constrained by the available space (a larger distance between the two occulters would increase performances). The interface with the hexapod was designed to place the bench optical axis at the same height as MOTA when the hexapod is in its centered configuration. The center of gravity of the bench is centered on the hexapod.

Most mechanical parts are made of aluminum, with either clear or black anodization. The two occulters are black anodized as they will be directly illuminated by MOTA.

4. SIMULATED PERFORMANCES

The MOTA + SLB configuration was modelized to verify the design and to check the experimental measurements against the theoretical predictions. The main contributors to the image seen on the SLB are the geometrical straylight generated inside MOTA and diffraction by the SLB occulters. The optical model was also used to evaluate the straylight from inside the SLB itself.

4.1. Geometric straylight

The geometric straylight was simulated using the FRED software. The model is illustrated on Figure 4-1.

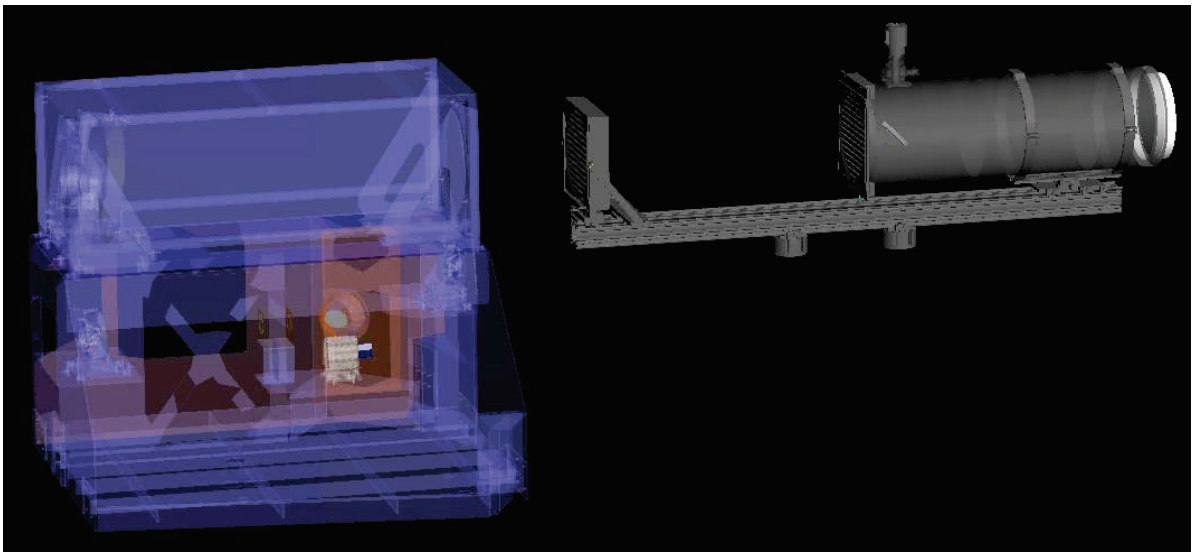

Figure 4-1 – Straylight bench in front of MOTA

Several simulations were performed on the model:

- A simulation with scattering in MOTA and no occulters or scattering on the straylight bench. This simulation was checked against MOTA's reference straylight simulations to ensure consistency.
- A simulation with scattering in MOTA, both occulters active but no scattering in the straylight bench. This simulation shows the result that can be expected if the straylight bench internal straylight is negligible.
- A simulation with scattering in both MOTA and the straylight bench. This is the main result that simulates the expected behavior of the system.

All the results presented here are divided by the reference irradiance from the reference simulation and plotted in log scale.

Figure 4-2 presents the reference simulation where the second occulter has been disabled: in the top half of the image, we see the black/white transition from MOTA directly imaged on the straylight bench's detector. Around the bright area, and especially in the bottom half of the picture, we can see MOTA straylight. Looking at the vertical cross-section, we see on the left that the straylight level decreases linearly (in log space) away from the transition, as expected from the Harvey-Shack model used here.

Note that the scene appears as a rectangle (and not a black/white transition) because the SLB's field-of-view is larger than the ±4.5mrad field-of-view of MOTA projected images.

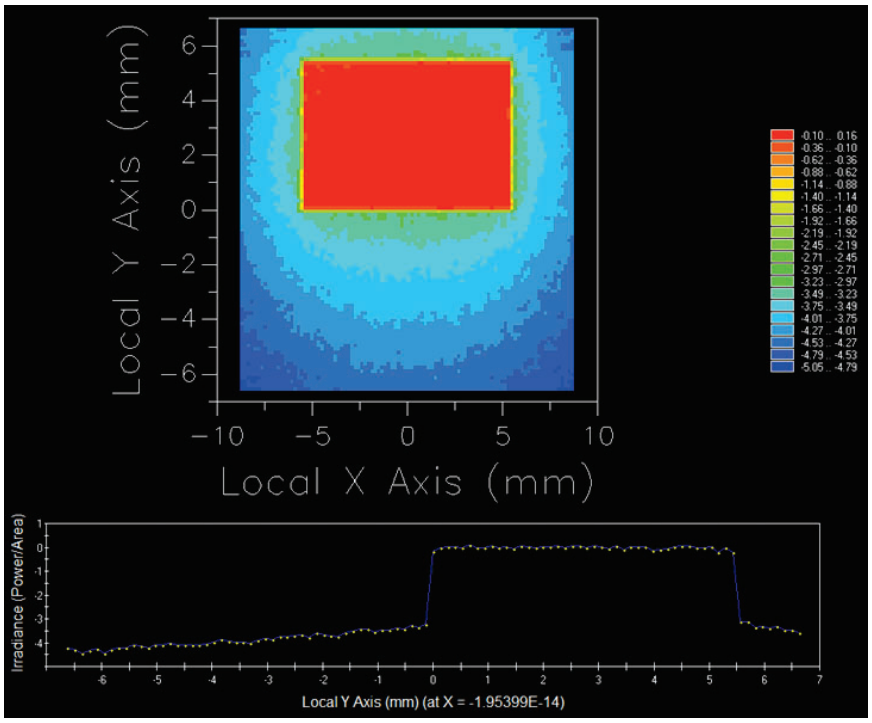

Figure 4-2 – FRED simulation, no back occulter, no scattering in the bench. Data normalized to Lmax, log10 scale.

Next, the second occulter is reactivated. Figure 4-3 presents, in log scale, the simulated image with and without scattering due to the straylight bench (log threshold set to -9.5, i.e. values at -9.5 are zero in linear scale).

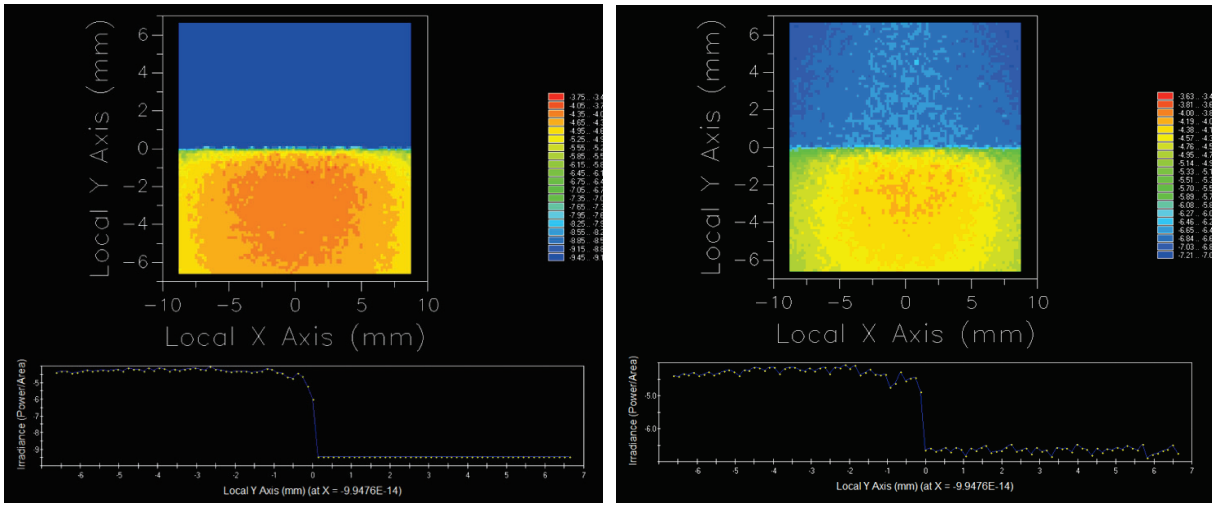

Figure 4-3 – FRED simulation. Data normalized to L_{max}, log10 scale.

Left: no scattering in the SLB. Right: scattering in the SLB.

As expected, the white half of the image is intercepted by the occulters, resulting in an image that appears inverted: the top half is dark while the bottom receives MOTA straylight.

In the image on the left where there is no scattering inside the straylight bench, the top half of the picture receives no light at all. Compared to Figure 4-2 we can also note that the shape of MOTA straylight has changed: it now appears relatively flat. This behaviour is expected from the field-dependent transmission of the occulting system (cf. Figure 2-2).

In the image on the right, the straylight from MOTA can be seen as before but the top half now receives some light: the straylight generated inside the bench, almost entirely due to scattering on the telescope mirrors.

Since only straylight from MOTA reaches these mirrors, the straylight observed here is “straylight of straylight”, i.e. (at least) twice scattered light, several order of magnitudes fainter than MOTA straylight.

Comparing the two images of Figure 4-3 we see that the “internal straylight” of the bench is over two orders of magnitude lower compared to the apparent level of MOTA’s straylight on the detector.

4.2. Diffraction

Diffraction from the occulters was simulated using a proprietary Matlab code. The core of the simulation simulates a plane wave that propagates through the SLB:

- A monochromatic plane wave is generated.
- The plane wave reaches the first occulter where it is partially transmitted.
- The transmitted field is Fresnel-propagated between the two occulters.
- The field that reaches the second occulter is once again partially transmitted.
- After the second occulter the field is Fraunhaufer-propagated since the telescope is infinity focused.

This core function was used to simulate a spatially and spectrally extended incoherent source representative of the MOTA experimental configuration. The result is illustrated on Figure 4-4. On this figure the 0mrad origin corresponds to the position of the black/white transition.

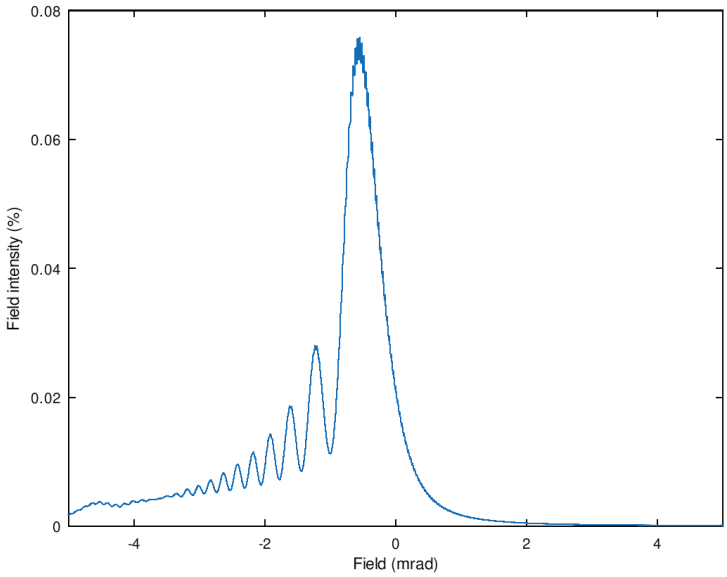

Figure 4-4 – Predicted diffraction pattern of the spatially and spectrally extended source, relative to the reference radiance.

From this simulation the diffraction pattern is expected to dominate MOTA straylight close to the transition. Further away both contributors are predicted to have a similar level.

4.3. Combination of the two contributors

The results from the two straylight contributors can now be combined. Since both effects are independent in the first order (a fraction of the diffraction figure will be due to diffracted MOTA straylight, but it will be 3-4 orders of magnitude smaller than diffraction of the bright fields) we simply sum the two datasets to obtain the final predicted image. Two points of attention:

- The FRED simulations were performed with large pixels to improve the SNR. In the final sum the oscillations seen on Figure 4-4 will not be as clear due to the rougher sampling.
- The diffraction simulations were only performed along one dimension. On the real images we expect to see additional (small) effects in the areas close to the corners of the bright square.

Figure 4-5 illustrates the final predicted result. The diffraction pattern dominates the center of the image, especially around the first peak. Noise due to scattering in MOTA can be seen in the dark fringes, further away from the transition zone, and in the areas not affected by diffraction.

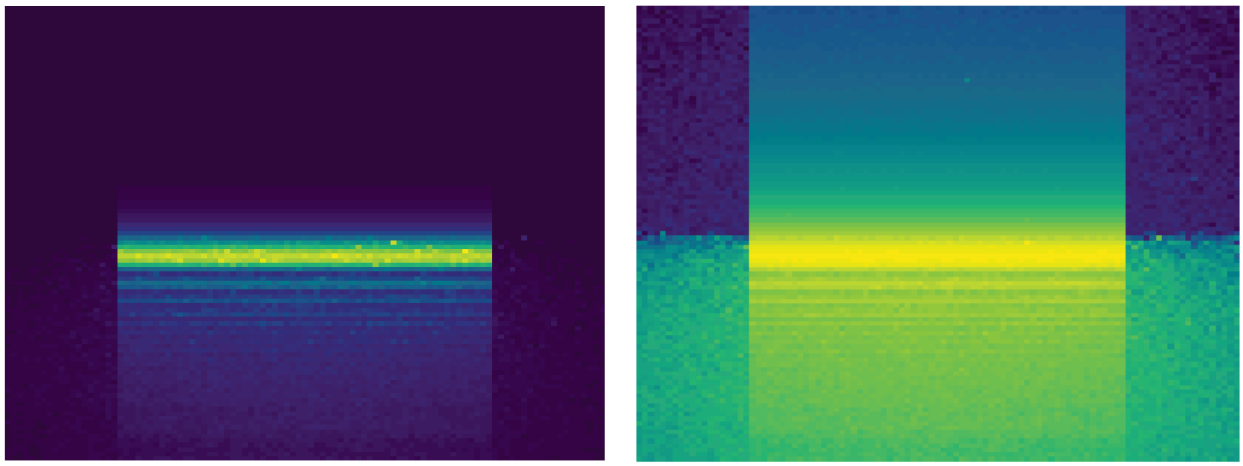

Figure 4-5 – Predicted result on the straylight bench in linear (left) and Log10 (right) scales

The log scale picture clearly shows the difference between the top part, that receives only straylight internal to the bench, and the bottom part that receives MOTA straylight. Outside the area of influence of the diffraction pattern, MOTA and the bench's straylight levels can be directly seen without impediment.

In Figure 4-6 (left) we plot the central column of the previous image and separate the two contributors to evaluate their respective weights. On the right side of the figure, we plot a column outside the area of diffraction. On both plots MOTA specification is displayed in red.

A note on the shape of the red area: MOTA straylight specification is a constant 0.08% (starting at +1mrad) of the brightfield level; the red area should apparently be a rectangle and not a triangle. The triangular shape is due to the SLB transmission varying linearly with the field being observed: at 0mrad the transmission is 0%, and it increases to 100% at +5mrad. This is a direct consequence of the occultation geometry, as can been seen on Figure 2-2. Consequently, the specification must be modified to take into account the attenuation of the apparent straylight close to the transition as we approach the transition.

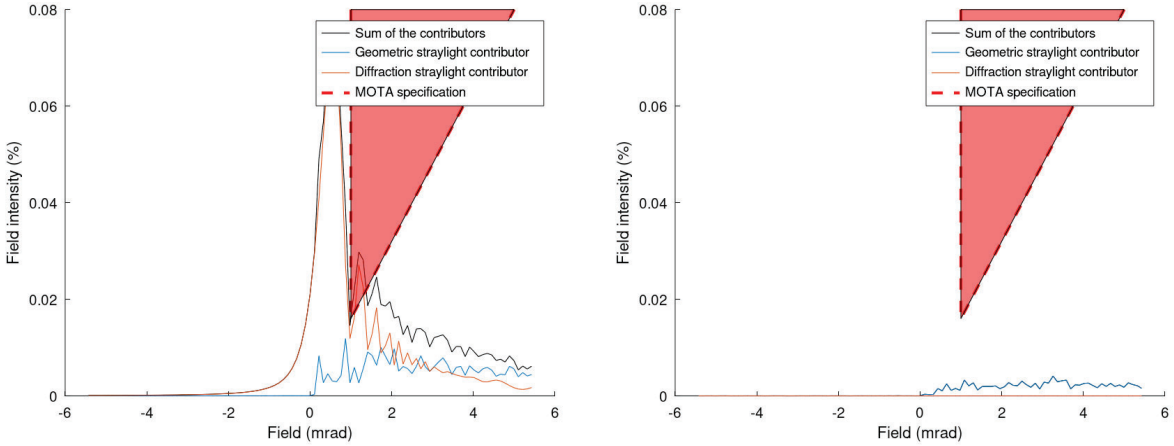

Figure 4-6 – Predicted result on the straylight bench, central column (left) and off-diffraction column (right), relative to L_{ref}

On the central column, except close to the transition, the two contributors are of the same order of magnitude. The effect of MOTA expected straylight can easily be seen on the sum: direct comparison of images taken during the lifetime of MOTA should give an indication of how MOTA straylight evolves with time. In addition, this measurement can be used to assess conformity to the requirement: if the measured level is lower than the specification's threshold level, the system is compliant. On the other hand, if the measured level is higher than the threshold no conclusion can be drawn without good confidence in the contribution of diffraction.

On the side column diffraction is absent. Only geometric straylight is present: on this area we have a direct indication of the level of straylight of both MOTA and the bench. MOTA relative straylight evolution can be followed during its lifetime by comparison of this area.

In addition, post-processing of either of these areas in the image should give an indication of the absolute level of straylight in the area of interest (assuming reasonably accurate diffraction, or geometric straylight models). Combining the data from both areas could further improve the absolute measurement.

5. EXPERIMENTAL RESULTS

Three sets of data were acquired: transition centered on MOTA field-of-view, and transitions at ±4.5mrad from the center. After acquisition the raw data was scaled to the reference radiance level and post-processed to mitigate the effects of diffraction. The post-processing method, not discussed here, has been validated on the simulated data generated in section 4. For each configuration the straylight is presented in linear and log scale as surface plots. In addition, for the central column of the detector we plot the data both before and after processing along with MOTA specification.

Figure 5-1 presents the result with the black/white transition centered on MOTA field-of-view. The straylight is presented in linear and logarithmic scale as surface plots on the left. On the right, for the central column of the detector we plot the data both before and after processing along with MOTA specification.

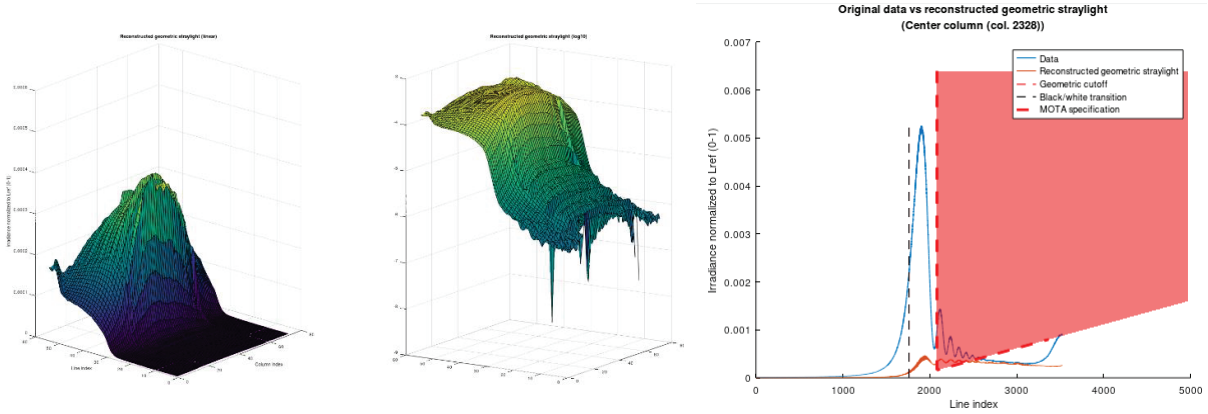

Figure 5-1 – MOTA reconstructed geometric straylight, transition centered on the field of view.

The processing algorithm is able, to a large extent, to separate the effect of diffraction from the effects of scattering, but there are some clear residual oscillations. There are two possible sources for these oscillations:

- A misalignment between the diffraction pattern and the detector lines. This source of error is proportional to the amplitude of diffraction.
- The scattered light originating from the diffraction figure itself as it reflects on the SLB mirrors. This straylight will also be additive and proportional to the amplitude of diffraction. Note that since there is little visible straylight in the occulted area of the detector (on the left half of the blue curve on Figure 5-1) or in the areas around the diffraction figure, this contributor clearly does not generate a constant background level.

The second source is unlikely: looking around line 3500 (far right portion of the plot), we see that the “bump” (which is actually a ghost) in the measured data is perfectly removed by the processing. This ghost would generate about the same amount of internal scattering as the third diffraction oscillation: if this was the dominant mechanism a small rebound in the reconstructed straylight would be seen. Consequently, the source of these residual oscillations is likely to be a slight misalignment between the black/white transition and the axis of the occulters (if it was due a misalignment between the occulters and the detector, we would also see this effect on the ghost at line 3500).

Both contributors being additive and proportional to the amplitude of diffraction, the straylight values computed here can be considered a higher bound. On Figure 5-2 we zoom in on the interesting part of the result.

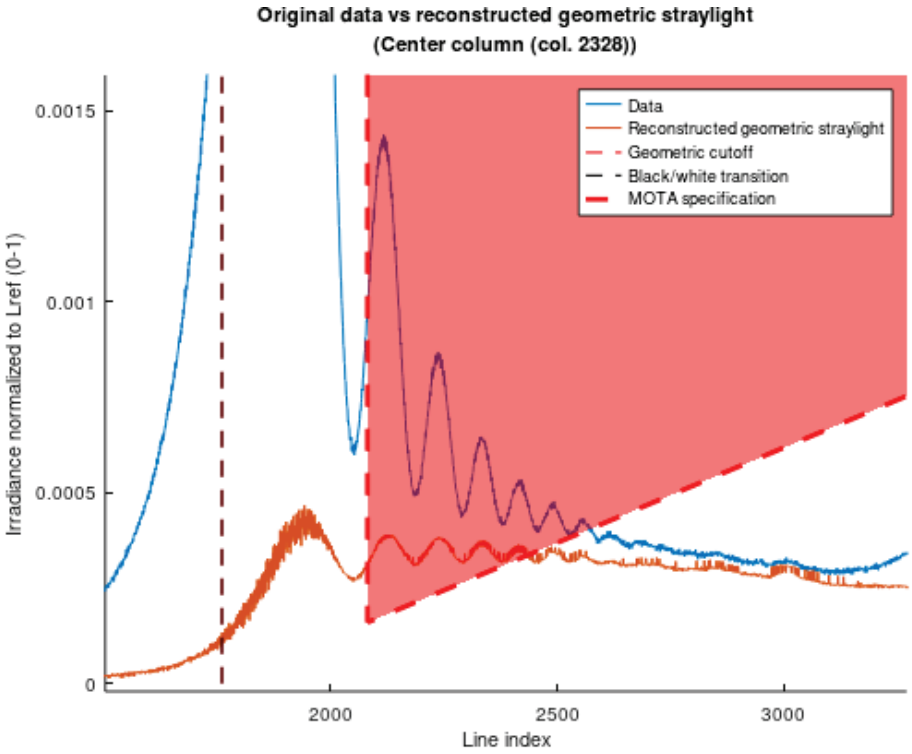

Figure 5-2 – Comparison of the two reconstruction methods.

These first results show that the SLB can be used as a relative measurement tool, capable of monitoring the evolution of MOTA straylight during its lifetime. The results here cannot be interpreted as absolute measurements at this time: the SLB error budget has not been established yet, and its behaviour near the transition is not well understood.

The absence of significant bench-internal straylight (which would be visible on the left portion of the plots) indicates that SLB-internal straylight is low, making it compatible with relative and absolute measurements, but other causes such as post-processing artifacts or as-yet unidentified effects could be at play and should be investigated before moving on to absolute measurements.

The SLB has been designed to be capable of absolute measurements. As a first step the relative measurement mode has been validated, and the ongoing work on the error budget will validate the accuracy of the absolute mode.

Figure 5-3 compares the reconstructed straylight levels measured at the three FOV positions to the simulations presented in section 4. The unprocessed data is not displayed to avoid clutter.

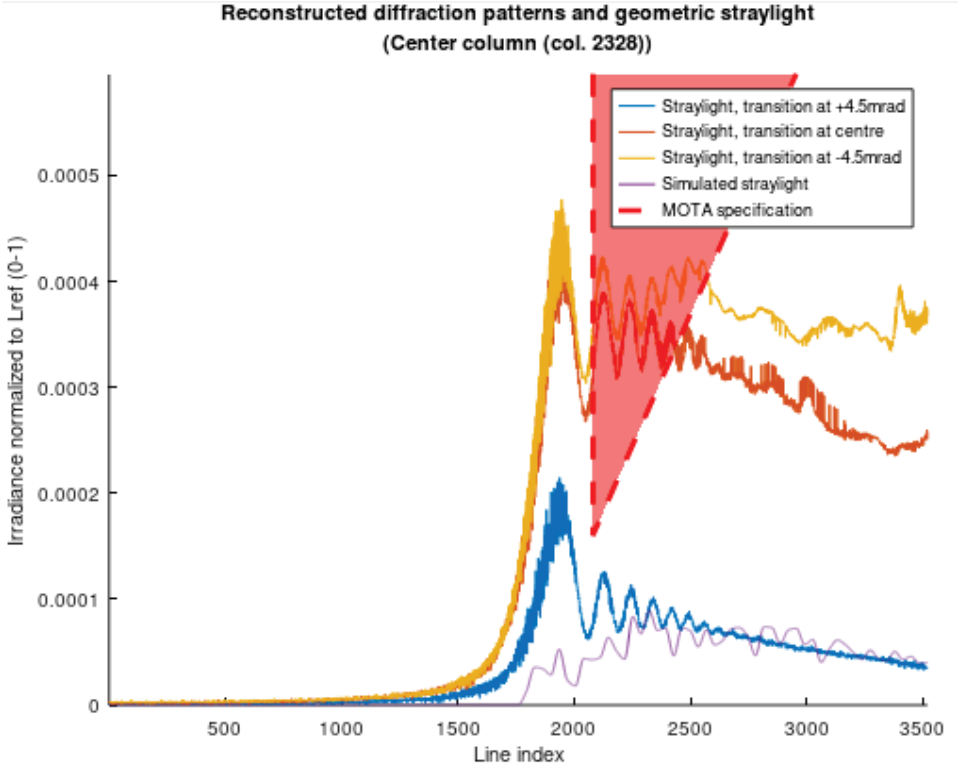

Figure 5-3 – Reconstructed vs simulated straylight

The straylight level at +4.5mrad is in very good agreement with the simulations that consider the nominal contamination of MOTA, while the levels at -4.5mrad and at the center are much higher. The level at -4.5mrad is ~20% higher than at the center (mainly visible far from the transition).

These differences are unlikely to be due to a high contamination (which would also be visible at +4.5mrad). It is more likely that in these two configurations some mechanical part inside MOTA is illuminated and seen from the bench, scattering additional light inside the field of view.

The (residual) diffraction patterns are well-aligned, an indication that the mismatch between the results in not due to a displacement of the occulters or some other misalignment.

The results show that the straylight level obtained have the same order of magnitude than the straylight levels predicted by simulation.

It has been observed that the measurements are different at +4.5mrad and at -4.5mrad and at the center.

Two hypotheses have been identified:

- Hypothesis 1: difference of position between the pattern plate and the fixed field diaphragm of the MOTA.
- Hypothesis 2: presence of a spectral filter inside MOTA intermediate pupil (added to have the measurements done at the same wavelength as the simulations. This hypothesis is less likely as this would have the same impact on the signal for each field of view.

The hypotheses have not been fully confirmed and some complementary analyses are needed.

It is important to note that we are talking here about extremely low level of signal and that the measurements stays in any case below the FCI straylight requirement.

In any case, it has been confirmed through this study and test campaign that the straylight level generated are in the expected range of values.

6. CONCLUSION

We have presented a new experimental straylight diagnostics setup, the Straylight Bench (SLB), to measure OGSE straylight. The measurement principle is based on external coronagraphy: the resulting system is simple and low-cost, notably using only commercial off-the-shelf optics. The system architecture includes a built-in self-check that can differentiate between the straylight that originates from inside SLB and from inside the OGSE under test.

This measurement principle was applied to the MOTA OGSE in NUST configuration. Scattering and diffraction simulations were performed to check the design and predict the experimental performances.
The test campaign showed that:

- the SLB behaviour closely matches the simulations,
- the SLB internal straylight (as seen by the self-check area of the sensor) is as expected and low enough to evaluate OGSE-type straylight levels,
- some additional measurements are necessary to better understand the SLB behaviour, especially close to the transition.

To consolidate the test results, some additional test campaign shall be performed to monitor the evolution of straylight level of MOTA.

The experimental results illustrate the power of this simple setup as a straylight diagnostics tool for high contrast scene optical equipment.

This document is issued within the framework of TRP Efficient Straylight Characterisation and Verification Techniques for Earth Observation Instruments awarded to the TNO & Thales Alenia Space – France consortium as well as an internal TAS funding.

Reference

[1] E. Compain, *et al.*, “VNIR, MWIR, and LWIR source assemblies for optical quality testing and spectroradiometric calibration of earth observation satellites”, *Proc. of Optical Design and Engineering VI*, vol. 9626, 962626 (2015)

[2] W. Glastre, *et al.*, "Description and performance of the OGSE for VNIR absolute spectroradiometric calibration of MTG-I satellites", *Proc. of SPIE*, Vol. 10562, 105624H (2017).

[3] P. Martin et al., FCI instrument on-board MeteoSat Third Generation satellite: design and development status , Proceedings Volume 11852, International Conference on Space Optics — ICSO 2020; 118520B (2021)

[4] J. Ouaknine et al., 17 November 2017 The FCI on board MTG : optical design and performances , Proceedings Volume 10563, International Conference on Space Optics — ICSO 2014; 1056323 (2017)

[5] Y. Durand et al?, The flexible combined imager onboard MTG: from design to calibration, Proceedings Volume 9639, Sensors, Systems, and Next-Generation Satellites XIX; 963903 (2015)

[6] J. Ouaknine, et Al., FCI PFM optical test results, Proceedings Volume 11852, International Conference on Space Optics — ICSO 2020; 118520A

[7] MTG Flexible Combined Imager optical design and performances, Proceedings Volume 8866, Earth Observing Systems XVIII; 88661A (2013)

[8] Koutchmy, Serge, “Space-borne coronagraphy”, *Space Science Reviews, Volume 47, Issue 1-2, pp. 95-143*